Int. J. Electrochem. Sci., 8 **(2013)** 2515 - 2523

International Journal of
ELECTROCHEMICAL
SCIENCE
www.electrochemsci.org

Electrochemical Behavior of the Titanium Plate with Carbon Films in a Vanadium Sulfate Solution

Huijun Liu[1], *Tingting Cai*[1], *Qiushi Song*[1], *Lingxu Yang*[1], *Qian Xu*[1,*], *Chuanwei Yan*[2]

[1] School of Materials Science and Metallurgy, Northeastern University, Shenyang, 110819, PR China.
[2] State Key Laboratory for Corrosion and Protection, Institute of Metal Research, Chinese Academy of Sciences, Shenyang 110016, PR China.
[*]E-mail: qianxu201@mail.neu.edu.cn

Received: 6 November 2012 / *Accepted:* 11 December 2012 / *Published:* 1 February 2013

A titanium plate with carbon films (TPCF) prepared by electrodeposition in a LiCl-KCl-K_2CO_3 melt is used as the electrode for vanadium redox flow battery. The electrochemical behavior of V^{2+}/V^{3+} and VO^{2+}/VO_2^+ redox couples on TPCF electrode is investigated by cyclic voltammetry, potentiodynamic polarization and impedance techniques. The results show that the V^{2+}/V^{3+} redox couple performs a quasi-reversible process on TPCF electrode. However, VO^{2+}/VO_2^+ redox couple presents an irreversible process. The carbon atoms on surface of TPCF electrode can be oxidized when the potential reaches 1.5 V, which means that the TPCF electrode has lower corrosion resistance than graphite electrode.

Keywords: Vanadium redox flow battery, carbon films, titanium plate, electrochemical behavior

1. INTRODUCTION

Vanadium redox flow battery (VRB) is a new energy storage device which is developed quickly in recent years due to its advantages such as large capacity, deep discharge capability, high reliability, no cross contamination and environmental friendliness [1-6]. However, there are still several issues which are needed to improve eventually for the commercial application of VRB, such as electrolyte stability, membrane permeability and electroactivity of the electrode materials [7-9]. At present, the low cost carbon-polymer composite and graphite felt are widely used as the bipolar plate and the electrode for VRB, respectively [7]. Usually, the carbon-polymer composite electrode has relatively high bulk resistivity and can be easily corroded when the anodically polarized potential on them is more positive than that of oxygen evolution, and this kind of heterogeneous corrosion may lead

to battery failure due to electrolyte leakage [10-12]. Therefore, The electrode with high electrical conductivity, acid-resistance and electrochemical stability is still desirable for VRB.

The carbon film coated Ti plate has a good electroconductibility and mechanical strength which are corresponding to the structure of carbon film and Ti substrate, respectively [13]. And most importantly, it also has good adhesion between carbon film and Ti substrate due to the Ti-O-C gradient in comparison with the carbon films obtained by some researchers [14-19]. In addition, it consists of amorphous and crystallized phases. Therefore, it will probably be a candidate for electrode in VRB. The aim of this study is to investigate the electrochemical behavior of TPCF electrode in the electrolyte of VRB by cyclic voltammetry, potentiodynamic polarization and impedance techniques.

2. EXPERIMENTAL

2.1 Chemicals

The electrolyte used in this study was 2 mol dm^{-3} H_2SO_4 and 2 mol dm^{-3} vanadyl sulfate ($VOSO_4$) aqueous solution, with the supporting electrolyte of 2 mol dm^{-3} H_2SO_4. All chemicals were of analytical grade and used as received without any purification, and de-ionized water was used for all experimental solutions.

2.2 Electrochemical measurements

All experiments were performed in a cell containing with about 0.3 dm^{-3} of 2 mol dm^{-3} H_2SO_4+2 mol dm^{-3} $VOSO_4$ electrolyte by a PARSTAT 2273-potentiostat/galvanostat/FRA at the room temperature. A three-electrode setup was utilized, in which the reference electrode was saturated calomel electrode (SCE), the counter electrode a graphite plate(4 cm×5 cm), and the working electrode a TPCF electrode with working area of 0.785 cm^2 exposed to the electrolyte, which was prepared by electro-deposition in a LiCl-KCl-K_2CO_3 molten salt in the previous study [20]. Electrochemical impedance spectroscopy (EIS) was conducted in a frequency range between 0.01 Hz and 100 kHz with the AC amplitude of 10 mV at different polarization potentials.

2.3 Characterization TPCF electrode

The surface morphology of TPCF electrode was examined by scanning electron microscopy (SEM; JSM-6360LV). X-ray photoelectron spectroscopy (XPS) was obtained with ESCALAB250 XPS (Thermo VG, USA) at 5.5×10^{-8} mbar. Al-Kα(1486.6 eV) was used as X-ray source at 15 kV of anodic voltage. Spectra were analyzed using Spectrum software (XPSPEAK41).

3. RESULTS AND DISCUSSION

Figure 1 shows the potentiodynamic polarization curves of the bare Ti and the TPCF electrodes in 2 mol dm^{-3} H_2SO_4 at the scan rate of 10 mV s^{-1}. This indicates that the free corrosion potential, E_{corr},

of the TPCF electrode is about 696 mV more positive than that of the bare Ti plate. It can be deduced that the carbon film may protect its substrate from anodic dissolution, and enhance its stability in 2 mol dm^{-3} H_2SO_4.

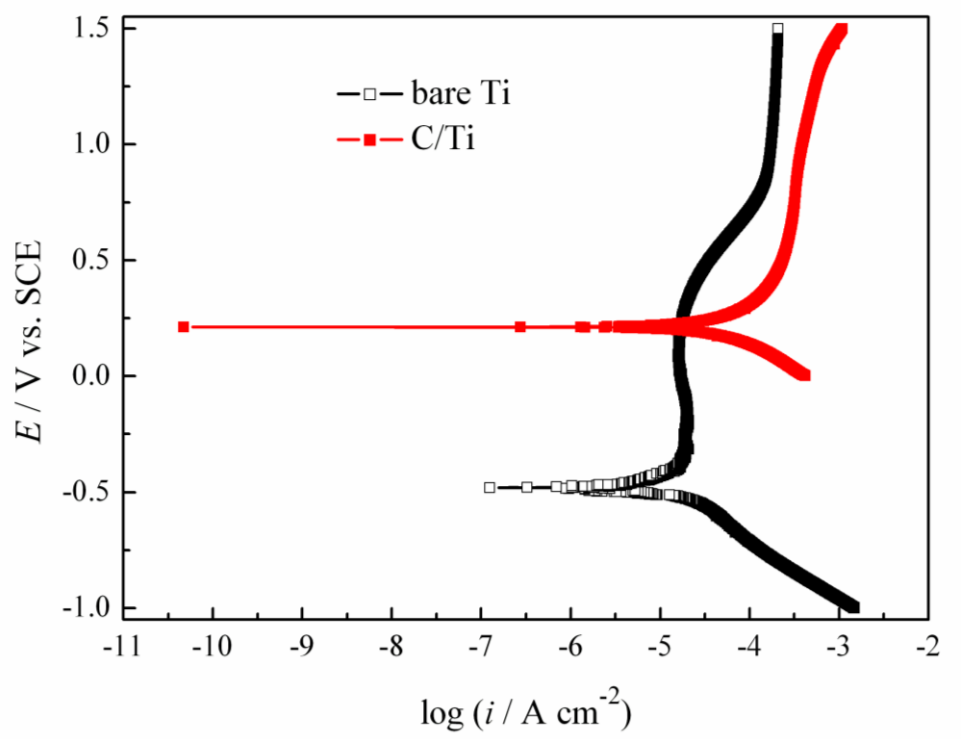

Figure 1. Potentiodynamic polarization curves of bare Ti and TPCF electrodes in 2 mol dm^{-3} H_2SO_4 at the scan rate of 10 mV s^{-1}

Figure 2 displays the cyclic voltammograms of TPCF electrode in 2 mol dm^{-3} H_2SO_4 +2 mol dm^{-3} $VOSO_4$ solution at the scan rate of 50 mV s^{-1}. A couple of peaks A1 and C1 are observed, which corresponding to the oxidation and reduction of V^{2+}/V^{3+}, respectively. A2 and C2 are associated with the oxidation and reduction of VO^{2+}/VO_2^{+}. The peak C2 can only be seen in the high resolution image shown in the insert, which means that the oxidation and reduction of VO^{2+}/VO_2^{+} presents an irreversible process on TPCE electrode. In addition, all of the peak value of current increases with scanning times. This may be because the surface of the carbon film was purged, which lead to an increasing in active area during the scanning process. The peak C0 at the potential of -0.9 V represents H_2 evolution.

The electrolyte of 2 mol dm^{-3} H_2SO_4+2 mol dm^{-3} V^{3+} was obtained by electro-reduction of 2 mol dm^{-3} H_2SO_4 +2 mol dm^{-3} $VOSO_4$ in the negative half-cell of a VRB. The cyclic voltammograms of TPCF electrode in 2 mol dm^{-3} H_2SO_4 +2 mol dm^{-3} V^{3+} under different scan rates are shown in Figure 3. It can be seen that the current peak for oxidation and reduction displays a high-degree of symmetry. As the scan rate increasing, the oxidation current peak (I_{pa}) and reduction current peak (I_{pc}) are also increases. The I_{pa} and I_{pc} are proportional to the scan rate (over the range of 25-75 mV s^{-1}).

Furthermore, the peak potential separation increases with the scan rate increasing. All of these indicate that the V^{2+}/V^{3+} redox reaction is a quasi-reversible process on TPCF electrode.

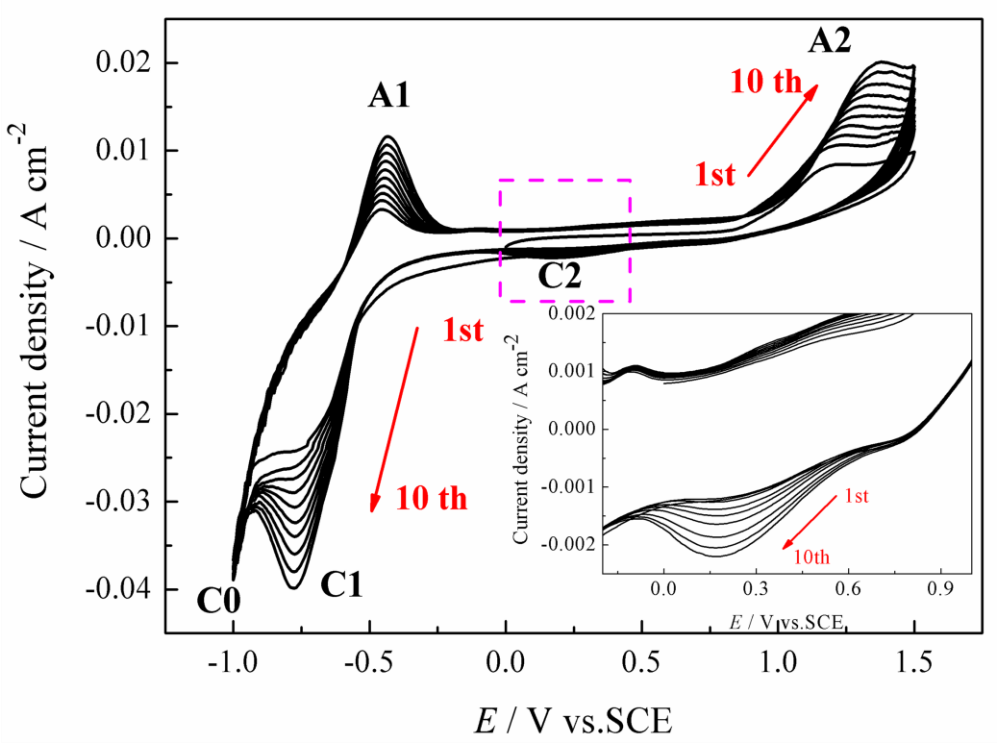

Figure 2. Cyclic voltammograms of TPCF electrode in 2 mol dm^{-3} H_2SO_4 +2 mol dm^{-3} $VOSO_4$ at the scan rate of 50 mV s^{-1}. The inset shows the corresponding curve of peak C2 at high resolution.

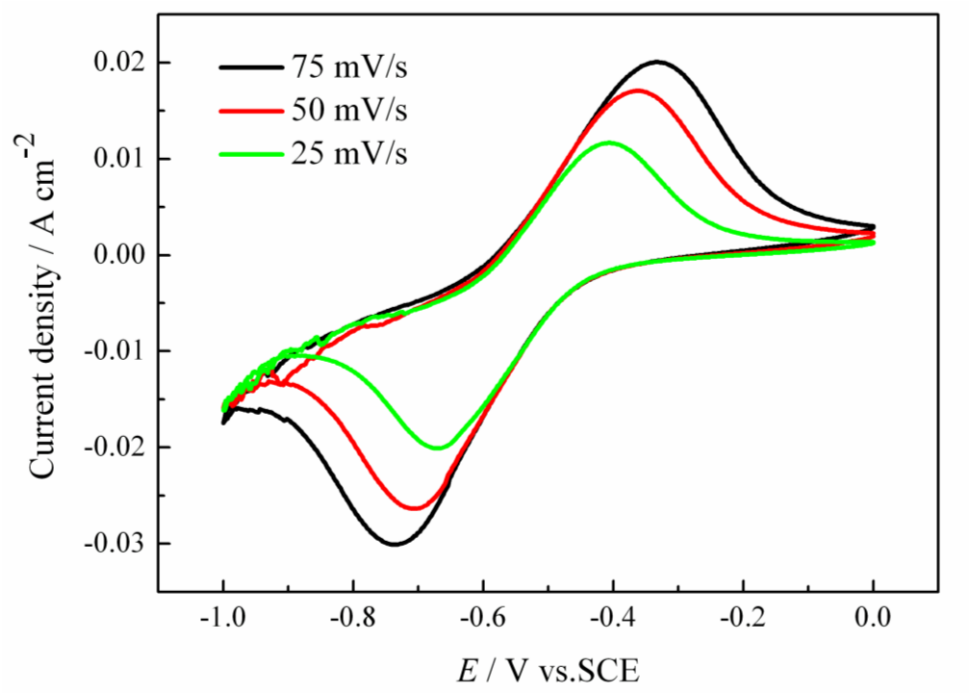

Figure 3. Cyclic voltammograms of TPCF electrode in 2 mol dm^{-3} H_2SO_4+2 mol dm^{-3} V^{3+} under different scan rates

Figure 4 shows the Nyquist plots of TPCF electrode in 2 mol dm^{-3} H_2SO_4+2 mol dm^{-3} V^{3+} under different potentials. The results show that the experimental curves present the shape of a semi-circle in the high frequency region, whereas it is a straight line with a slope of unity approximately in the low frequency region. The semi-circle is due to the combination of the double layer capacitance and the charge transfer reaction which is associated with reduction of V^{3+} ions [21]. This indicates that the reduction of V^{3+} on TPCF electrode is a mixed kinetic-diffusion controlled process in 2 mol dm^{-3} H_2SO_4+2 mol dm^{-3} V^{3+} in the polarization potential range between -0.425 V and -0.500 V.

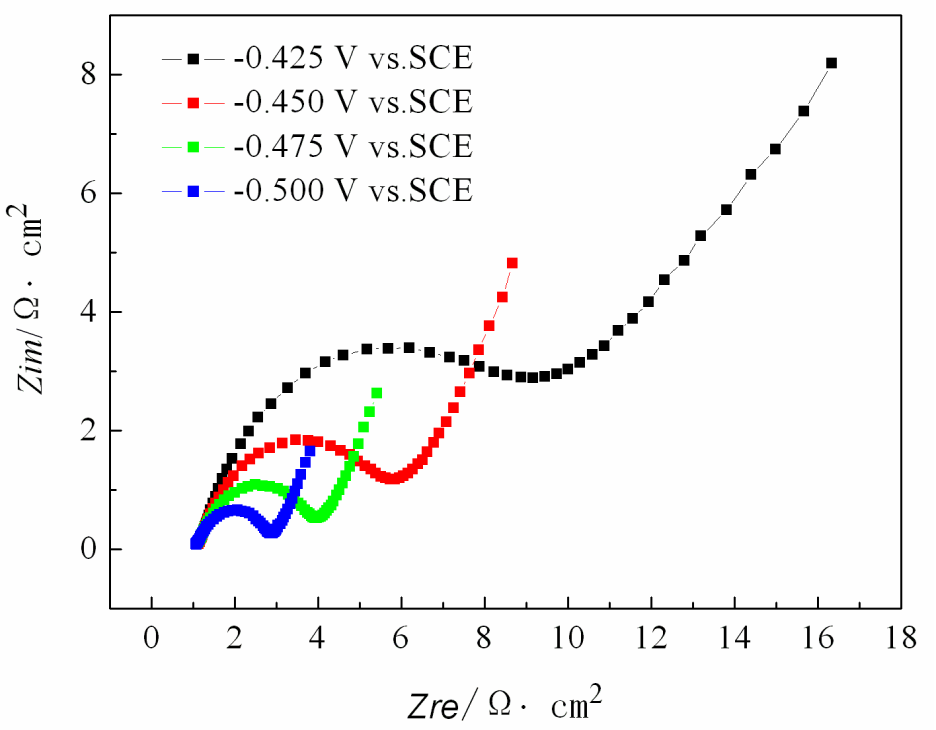

Figure 4. Nyquist plots of TPCF electrode in 2 mol dm^{-3} H_2SO_4+2 mol dm^{-3} V^{3+} under different polarization potentials

The battery-charging process is simulated by using potentiostatic polarization at 1.2 V and 1.5 V vs. SCE to investigate the electrochemical stability of TPCF electrode. The SEM images and digital picture of the surface on TPCF electrode before and after simulation of charging process are shown in Figure 5. The results show that there is no obvious change on surface morphology of TPCF electrode when the potential lower than 1.2 V by comparison of Figure 5a and Figure 5b. However, when the potential reaches 1.5 V, the TPCF electrode can be degraded severely as shown in Figure 5c, which may be due to the carbon atoms oxidized by high activity oxygen-atom. Figure 5d-f shows the SEM images with different magnifications of TPCF electrode after charging at 1.5 V for 3 h. This means that the TPCF electrode has lower corrosion resistance than graphite electrode at the same potential [10], which may be due to the prepared carbon film consists of amorphous and crystallized phases and the amorphous phase of carbon has higher electrochemical activity and can be easily oxidized to CO_2 than graphite electrode[20].

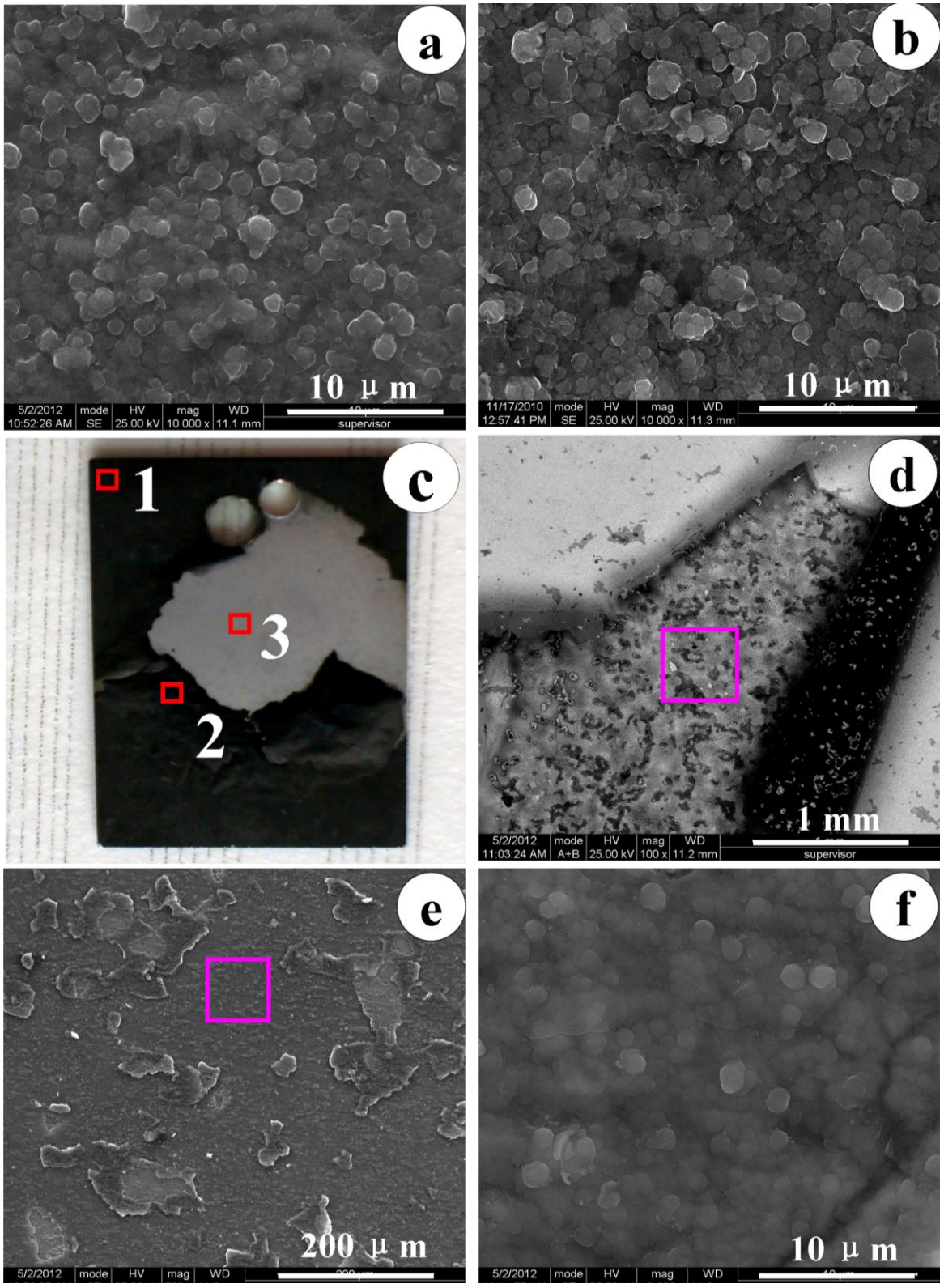

Figure 5. The SEM images and picture of TPCF electrodes before and after simulation of charging process a: before charging process; b: after charging at 1.2 V for 3 h; c: the picture for TPCF electrode after charging at 1.5 V for 3 h; d, e, f: SEM images with different magnifications of TPCF electrode after charging at 1.5 V for 3 h

Figure 6 shows the XPS spectra at different position of TPCF electrodes before and after simulation for charging process at 1.5 V for 3 h. The results show that after charging, the intensity of the O1s peak at the binding energy of 532 eV increases. In addition, the O content and the O/C ratio reach up to 27.8% and 0.38, compared to 22.2% and 0.28 of the TPCF electrode, respectively. This indicates that the carbon atoms on surface of TPCF electrode were oxidized during charging process and this is in agreement with SEM images as shown in Figure 5. Spectrum 3 corresponding to position 3 shown in Figure 5c, there appears a Ti2p peak at the binding energy of 456 eV besides the O1s and C1s peaks at the binding energy of 532 and 284 eV.

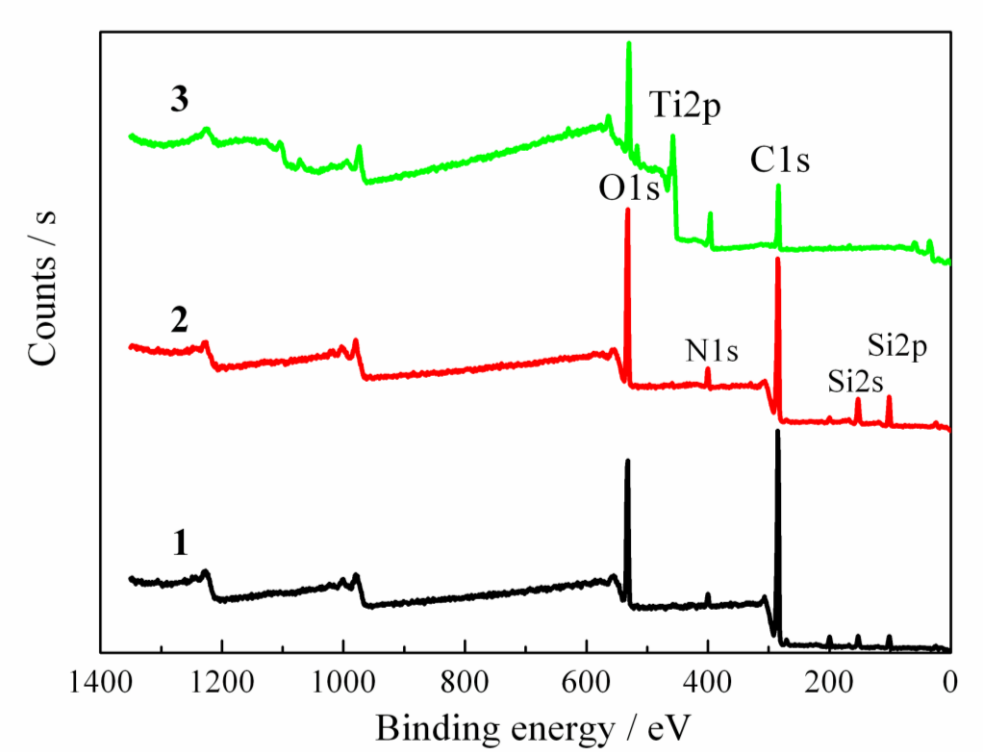

Figure 6. XPS spectra of TPCF electrode before and after simulation for charging process at 1.5 V for 3 h. Curves 1, 2 and 3 were corresponding to the XPS spectra of position 1, 2 and 3 shown in Figure 5(c).

The representative XPS C1s and Ti2p spectra of TPCF electrodes before and after simulation for charging process at 1.5 V for 3 h are fitted, and the results are shown in Figure 7. It can be seen that the intensity of functional group of C-O increases during charging process at 1.5 V by comparison of Figure 7a and 7b, which indicates that the carbon atoms on surface of carbon film are oxidized during charging process at 1.5 V and this is in agreement with SEM images shown in Figure 5. In addition, by combination of Figure 7c and 7d, a layer of TiC can be deduced to exist between the carbon film and the substrate, which may play a key role to prevent titanium from corrosion.

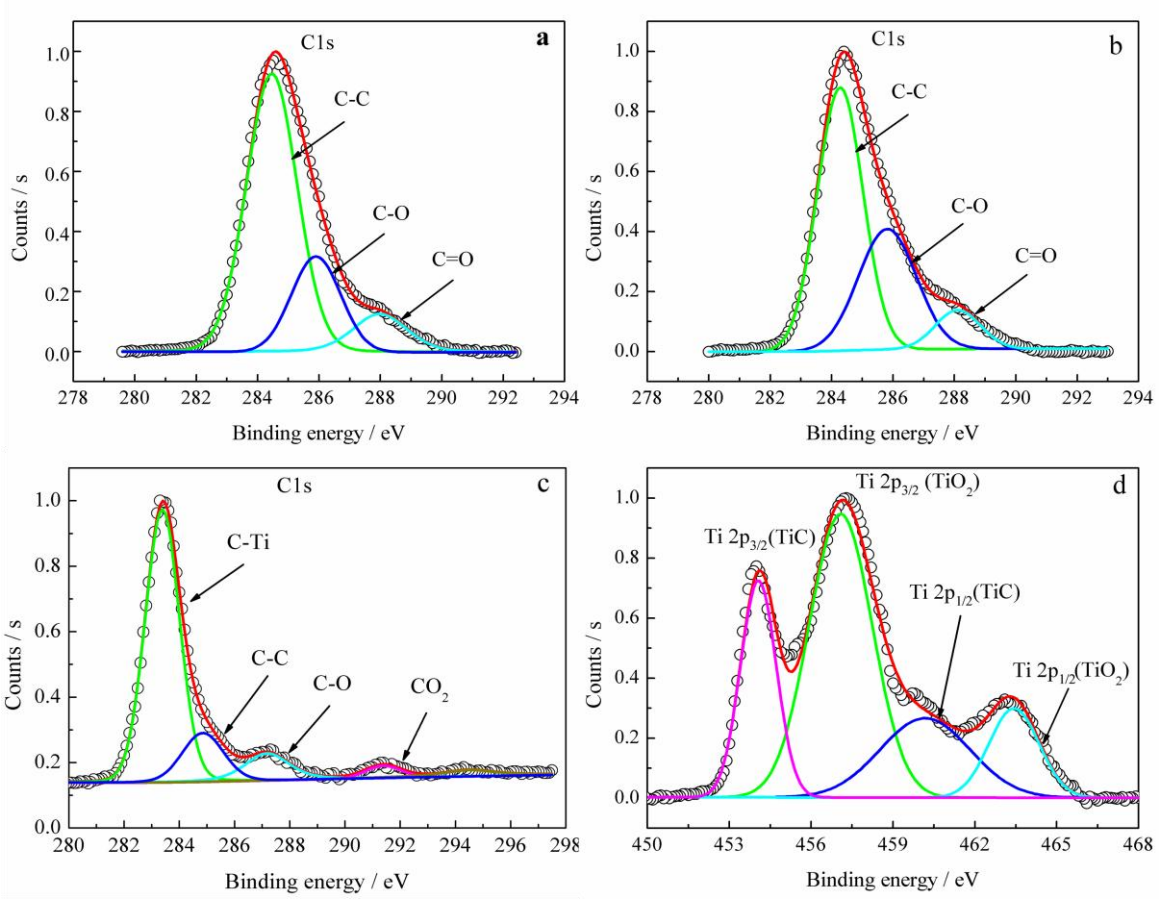

Figure 7. C1s and Ti2p high resolution XPS spectra of TPCF electrode at different positions in Figure 5(c). a: position 1; b: position 2; c and d: position 3

4. CONCLUSIONS

The electrochemical behavior of V^{2+}/V^{3+} and VO^{2+}/VO_2^{+} redox couple on the TPCF electrode, which was prepared by the electro-deposition in a LiCl-KCl-K_2CO_3 molten salt, is studied. The results show that the V^{2+}/V^{3+} redox couple performs a quasi-reversible process on TPCF electrode. However, VO^{2+}/VO_2^{+} redox couple presents an irreversible process. The carbon atoms on surface of TPCF electrode can be oxidized when the potential reaches 1.5 V, which lead to carbon film discontinuous. However, there is no obvious change at 1.2 V. In conclusion, the TPCF electrode still has some shortages to be used as the electrode for VRB. However, it can be used as the electro-bipolar plate when the applied potential difference is strictly controlled in VRB.

ACKNOWLEDGMENTS

The authors acknowledge National Natural Science Foundation of China (Grant No.50874026) and the financial support of Natural Basic Research Program of China (Grant No.2010CB227203) and the Fundamental Research Funds for the Central Universities (Grant No.N100602009).

References

1. E. Sum, M. Rychcik, and M. Skyllas-Kazacos, *J. Power Sources*, 16 (1985) 85
2. E. Sum, and M. Skyllas-Kazacos, *J. Power Sources*, 15 (1985) 179
3. C. Fabjan, J. Garche, B. Harrer, L. Jo¨rissen, C. Kolbeck, F. Philippi, G. Tomazic, and F. Wagner, *Electrochim. Acta*, 47 (2001) 825
4. P. Leung, X.H. Li, C.P. Leo´n, L. Berlouis,C. T. John Low, and F.C. Walsh, *RSC Advances*, 2, (2012) 10125
5. M. H. Chakrabarti, R. A. W. Dryfe, and E. P. L. Roberts, *Electrochim. Acta*, 52 (2007) 2189
6. L. Joerissen, J. Garche, C. Fabjan, and G. Tomazic, *J. Power Sources*, 127 (2004) 98
7. M. Skyllas-kazaocs, and M. Rychcik, *J. Power Sources*, 19 (1987) 45
8. M. Skyllas-Kazaocs, M. H. Chakrabarti, S. A. Hajimolana, F. S. Mjalli, and M. Saleem, *J. Electrochem. Soc.*, 158 (2011) R55
9. C. K. Jia, J. G. Liu, and C. W. Yan, *J. Power Sources*, 195 (2010) 4380
10. H. J. Liu, Q. Xu, C. W. Yan, and Y. L. Qiao, *Electrochim. Acta*, 56 (2011) 8783
11. V. Haddadi-Asl, and M. S.Rabbani, *Iranian Polymer Journal*, 7 (1998) 185
12. P. Qian, H. M. Zhang, J. Chen, Y. H. Wen, Q. T. Luo, Z. B. Liu, D. J. You, and B. L. Yi, *J. Power Sources*, 175 (2008) 613
13. Q. S. Song, Q. Xu, and C. Y. Xing, *Electrochem. Commun.*, 17 (2012) 6
14. G. S. Wu, L. L. Sun, W. Dai, L. X. Song, and A. Y. Wang, *Surf. Coat. Technol.*, 204 (2010) 2193
15. A. Afshar, M. Yari, M. M. Larijani, and M. Eshghabadi, *J. Alloys Compd.*, 502 (2010) 451
16. Y. Show, M. Miki, and T. Nakamura, *Diamond Relat. Mater.*, 16 (2007) 1159
17. J. Choi, S. Nakao, and J. Kim, *Diamond Relat. Mater.*, 16 (2007) 1361
18. L. F. Bonetti, G. Capote, L. V. Santos, E. J. Corat, and V. J. Trava-Airoldi, *Thin Solid Films*, 15 (2006) 375.
19. N. Yamauchi, N. Ueda, and A. Okamoto, *Surf. Coat. Technol.*, 201 (2007) 4913
20. Q. S. Song, Q. Xu, W. Yang, X. J. Shang, and Z. Y. Li, *Thin Solid Films*, 520 (2012) 6856
21. H. J. Liu, Q. Xu, C. W. Yan, Y. Z. Cao, and Y. L. Qiao, *Int. J. Electrochem. Sci.*, 6 (2011) 3483